



Research Paper / Makale

Stability Analysis of Rotating Blade Vibrations Using Lyapunov Exponents

Tarık KUNDURACI*

Department of Electricity and Energy, Akhisar Vocational High School, Manisa Celal Bayar University, 45200
Akhisar, Manisa, Turkey; tarik.kunduraci@cbu.edu.tr

Received/Geliş: 20.09.2017

Revised/Düzeltilme: 27.10.2017

Accepted/Kabul: 31.10.2017

Abstract: This paper presents an analysis of the vibration stability of a rotating blade due to shaft torsional vibration excitation. The governing equation adopted in the study is a Hill's type linear second order ordinary differential equation with multiple harmonically variable coefficient terms. The differential equation of the system is rewritten as two coupled first order ordinary differential equations. The stable and unstable regions are determined by the Lyapunov characteristics exponents on parameter space (grid) relating to the rotor speed, the torsional vibration excitation frequency and the blade natural frequency. The results are contrasted to those obtained by the strained parameter method (a perturbation technique), an excellent match is observed for small torsional vibration amplitudes ϵ .

Keywords: Chaos, Nonlinear Dynamics, Lyapunov Exponents, Rotating Blade Vibration, Stability.

**Lyapunov Üstelleri Kullanılarak Dönen Bir Bıçağın Titreşimlerinin
Stabilite Analizi**

Özet: Bu makalede, dönen bir bıçağın titreşim kararlılığının mil titreşim uyarılmasına bağlı olarak analizi sunulmaktadır. Çalışmada kullanılan temel denklem, birden fazla harmonik olarak değişken katsayı terimine sahip Hill tipi doğrusal ikinci dereceden adi diferansiyel denklemdir. Sistemin diferansiyel denklemi, iki birleşmiş birinci mertebeden adi diferansiyel denklem olarak yeniden yazılmıştır. Kararlı ve kararsız bölgeler, rotor hızına, burulma titreşim uyarılma frekansına ve bıçak doğal frekansına ilişkin parametre uzayındaki Lyapunov karakteristik üstelleri tarafından belirlenir. Sonuçlar, genişletilmiş parametreler yöntemiyle (bir pertürbasyon tekniği) elde edilenlerle karşılaştırıldığında, ϵ küçük burulma titreşim genlikleri için mükemmel bir eşleşme gözlemlenmiştir.

Anahtar kelimeler: Kaos, Lineer olmayan dinamik, Lyapunov Üstelleri, Dönen Bıçak Titreşimi, Stabilite.

1. Introduction

In complex dynamical systems, one way to exhibit the stable and unstable regions of the solution of the differential equation that represents the system is to calculate the Lyapunov characteristics exponents (LCEs). This paper aims to reproduce the stability charts formed by perturbation methods and numerical simulations by using alternative method of LCEs. Rotating blade vibration was recognized as one major cause of failure in turbomachinery that put a growing demand on more thorough analysis at the design stage. One problem that deserves more attention is the problem of blade vibration instability due to torsional vibration excitation. A study that results in a stability map for the shaft-blade design is extremely valuable for designers, diagnostics, and maintenance

How to cite this article

Kunduraci, T., "Stability Analysis of Rotating Blade Vibrations Using Lyapunov Exponents" El-Cezeri Journal of Science and Engineering, 2018, 5(1); 11-23.

Bu makaleye atıf yapmak için

Kunduraci, T., "Lyapunov Üstelleri Kullanılarak dönen bir bıçağın titreşimlerinin stabilite analizi" El-Cezeri Fen ve Mühendislik Dergisi 2018, 5(1); 11-23.

engineers. The importance of blade vibration was highlighted by A.V. Srinivasan [1] in his survey on the vibration of bladed disk assemblies. He classified blade vibrations into two categories; namely (i) structure induced vibration and (ii) aero-elastic induced vibrations.

The survey was mainly concerned with the structural induced vibrations and their modeling. The effect of stagger angle on the inertial and elastic coupling in bladed disks was reported by Crawley and Mokadam [2]. Tang and Wang [3] proposed a model for rotor fuselage dynamic analysis. The problem of blade vibration and its interaction with the main rotor torsional vibration was studied by Okabe et al. [4]. They showed that it is necessary to model both blade bending vibration and main rotor torsional vibration in turbomachinery. The authors adopted the modal synthesis procedure in their model by modeling the blade as a simple mass-spring subsystem and the shaft torsional flexibility as another discrete subsystem. The two subsystems were coupled and the natural frequencies were analyzed. The model-produced natural frequencies were compared to the actual measurement and close agreement was reported. Huang and Ho [5], the results of a study on the coupled shaft torsional and blade bending vibrations of a rotating shaft-disk-blade unit were presented. The shaft torsional and blade bending deformations were modeled using the Assumed Modes Method (AMM).

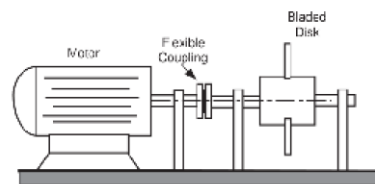


Figure 1. Schematic diagram of blade-disk-shaft system, Al-Bedoor (2001).

The study identified the nonlinear interaction and the destabilizing effect that the blade and shaft could introduce to excite each other. Due to the difficulty encountered in quantifying the nature of nonlinear coupling when the finite element method is used, a reduced-order nonlinear dynamic model for shaft-torsional and blade-bending vibrations that adopted the AMM to approximate blade deformations was presented by Al-Bedoor [6]. The simulation results showed that (i) the torsional vibration of the rotor system works as an excitation to the blade, (ii) some certain combinations of blade-shaft parameters can lead to unstable blade vibration and (iii) there is no explicit criteria for identifying exact combinations of parameters that can lead to unstable vibrations. Al-Nassar and Al-Bedoor [7] extracted an equation from the general solution developed by Al-Bedoor [6]. This extracted equation was converted into a general Mathieu equation whose solutions show the dynamic behavior of the blade under the effect of torsional vibration excitation.

In this work, the chaotic behavior of the governing equation developed by Al-Nassar et al. [8] was investigated. The Lyapunov exponents of the dynamical system were computed by using a numerical scheme proposed by Chen et al. [9]. The numerical approach is based on a time integration and is computationally efficient. It was shown that the maximum Lyapunov exponent was shown to have positive values for unstable regions, which indicates a chaotic motion of dynamical system under consideration. However, it is nearly zero for stable regions. Therefore, it is worth noting that the obtained Lyapunov spectrum is in agreement with the theoretical results obtained by Al-Nassar et al. [8].

2. The Governing Equation

A disk-shaft-blade system driven by an electrical motor is shown in Fig.1. The disk is assumed to be rigid and flexible blades are attached radially to the disk. The radius of the disk is R_D . The

coordinate system for the consideration is also shown in Fig.2. XY is the inertial frame, $x^m y^m$ is a body coordinate system of the motor shaft, $x^d y^d$ is a body coordinate system of the disk and $x^b y^b$ is the blade coordinate system which is attached to the root of the blade. x^b is always directed along undeformed blade centerline.

The dynamic model of a blade-disk-shaft system shown in Fig. 1 was used in this study. The equation of blade modal vibration can be written in the form

$$m_{q\theta}\ddot{\theta} + m_{q\theta}\ddot{\psi} + m_{qq}\ddot{q} + C_{q\theta}\dot{\theta} + C_{qq}\dot{q} + k_{qq}q = F_q \quad (1)$$

where opened and detailed forms of the factors are given by Al-Bedoor and Al-Qaisia [10].

The degrees of freedom are the rigid body rotation θ , the torsional deflection ψ and the blade modal deflection q . By considering only the blade model degree of freedom and under the assumptions of constant rotating speed $\dot{\theta} = \Omega$, and the square of the torsional deflection is small $\psi^2 \approx 0$, the following equation can be written:

$$(h + \psi q)\ddot{\psi} + \ddot{q} + 2\psi\dot{\psi}\Omega + (2\psi\dot{\psi} + 2\eta\omega_B)\dot{q} + (\omega_B^2 + C_1(\dot{\theta} + \dot{\psi})^2 + \dot{\psi}^2)q = 0. \quad (2)$$

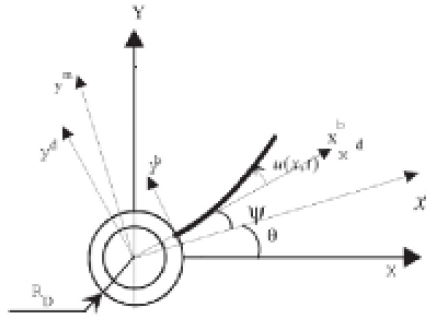


Figure 2. The coordinates system.

Here h and C_1 are constants depending on blade bending mode and ω_b is the blade natural frequency. As mentioned in ref. [8], C_1 can be taken as unity. The first term in Eq.(2) stands for part of dynamic coupling between the shaft torsional degree of freedom and the blade bending modes. The second term is blade modal acceleration and third term is a function of torsional degree of freedom parameters which can also be taken as a forcing term. The blade damping terms are shown in fourth term in Eq.(2) where η represents the structural damping and $2\psi\dot{\psi}$ stands for the effect of torsional vibration.

It is possible to write rotor torsional deflection as

$$\psi = \varepsilon \sin \omega t$$

where ε is a small parameter and indicates the small order of torsional vibration, ω is the torsional excitation frequency. The equation of motion reduces to the following form if one substitutes ψ and $\dot{\psi}$ into Eq.(2)

$$\ddot{q} + P_1(t)\dot{q} + P_2(t)q = f(t) \quad (3)$$

This is a second order differential equation with respect to $q(t)$ having variable coefficients. In this equation,

$$\begin{aligned} P_1(t) &= \varepsilon^2 \omega \sin 2\omega t + 2\eta\omega_B, \\ P_2(t) &= \omega_B^2 + \Omega^2 + \frac{1}{2}\varepsilon^2 \omega^2 + 2\varepsilon\omega\Omega \cos \omega t + \frac{3}{2}\varepsilon^2 \omega^2 \cos 2\omega t, \\ f(t) &= \varepsilon h\omega^2 \sin 2\omega t - \varepsilon^2 \omega\Omega \sin 2\omega t. \end{aligned}$$

If one uses the transformation

$$q = x \exp\left(-\frac{1}{2} \int P_1(t) dt\right)$$

and considers the homogeneous part of Eq.(3), the system reduces to the following form

$$\ddot{x} + P(t)x = 0 \quad (4)$$

where

$$P(t) = P_2 - \frac{1}{2}P_1^2 - \frac{1}{2}\dot{P}_1^2.$$

It is convenient to rewrite the governing equation in non-dimensional form. To do this, one can define first the dimensionless frequencies $r_1 = \omega_B/\omega$ and $r_2 = \Omega/\omega$ which are independent to each other and govern the stability of the system. Second, using the transformation

$$\tau = \frac{1}{2}\omega t$$

Eq.(4) becomes

$$x'' + \left(\delta + 8\varepsilon r_2 \cos 2\tau + 2\varepsilon^2 \cos 4\tau + \frac{1}{2}\varepsilon^4 \cos 8\tau\right)x = 0 \quad (5)$$

where double prime denotes the differentiation with respect to dimensionless time variable τ and $\delta = 4(r_1^2 + r_2^2) + \frac{3}{2}\varepsilon^2$. Here the term due to damping is neglected.

3. Numerical Calculation of LCEs

The Lyapunov characteristic exponents(LCEs) play a crucial role on determining the behavior of dynamical systems. Because of the strong dependence on initial conditions, one may compute LCEs of a corresponding dynamical system to understand how it evolves in time and want to check if it has a chaotic manner. An n -dimensional autonomous smooth dynamical system can be characterized by a differential equation as

$$\dot{x} = \frac{dx}{dt} = F(x), t > 0 \quad (6)$$

Here F is a continuous function on an open set $U \subset \mathbb{R}^n$ and has continuous derivatives on the same set [11]. $x(t)$ is the state vector at time t . A non-autonomous system could be rewritten as an autonomous system by adding the *time* as a dependent variable ($dt/dt = 1$). So the dimensionality increases by one. It is possible to make the above description for discrete dynamical systems rewriting the state equation as

$$x_{t+1} = f(x_t) \quad (7)$$

where t is now a natural number, f maps x_t to x_{t+1} . Starting with an initial condition x_0 , the repeated iterations of f will produce a discrete set of points namely an orbit in phase space.

3.1 Computation of LCEs

Let us assume that the dynamical system under consideration is described by the ordinary differential equation system (6). Differentiating with respect to the initial condition x_0 , we derive the n^2 -dimensional ordinary differential equation system [9]

$$\dot{Y} = J(x(t))Y \quad (8)$$

where I_n denotes the $n \times n$ identity matrix and $J(x)$ the Jacobian matrix of f . Now let us consider the evolution of an infinitesimal n -parallelepiped with the axis $p_i(t) = Y(t)p_i(0)$ for $i = 1, \dots, n$, where $p_1(0), \dots, p_n(0)$ denotes an orthogonal basis of the phase space. The i th Lyapunov exponent, which measures the long-time sensitivity of the flow $x(t)$ with respect to the initial data x_0 at the direction $p_i(t)$, is defined by the expansion rate of the length of the i th axis $p_i(t)$. The i th exponent can be calculated as the time evolution limit of the natural logarithm of the rate; briefly,

$$\lambda_i = \lim_{t \rightarrow \infty} \ln \left| \frac{p_i(t)}{p_i(0)} \right|. \quad (9)$$

Without loss of generality, the direction $p_i(t)$ can be chosen as the i th column of the identity matrix I_n . Thus if the Gram-Schmidt (QR) reorthonormalization procedure proposed in refs. [12,13] is used for $Y(t)$ in the form

$$Y(t) = Q(t)R(t), \quad (10)$$

the orthonormal matrix $Q(t)$ is uniquely defined and an upper triangular matrix $R(t)$ with positive diagonal entries $R_{i,i}(t)$. Therefore, with these assumptions, it is possible to introduce the alternative definition for Lyapunov exponents [13],

$$\lambda_i = \lim_{t \rightarrow \infty} \frac{1}{t} \ln R_{i,i}(t). \quad (11)$$

The presence of the limit in Eq.(11) basically depends on the fundamental theorem of ergodic dynamical systems [14]. The numerical computation of Lyapunov exponents are well developed as described by Benettin et al. [15] where the numerical algorithm uses a discrete QR algorithm. Some

additional successful developments of continuous algorithms in computing Lyapunov exponents are available in literature[16,17]. Here we will use a simple discrete QR algorithm proposed in [9] where the detailed explanation of the algorithm can be found. For a given time interval $[0, T]$ the mesh points could be t_0, t_1, \dots, t_M where $t_i = ih$. The step-size h is calculated from the rate of $\frac{T}{M}$. For sufficiently small h values, the approximate solution for $Y(t)$ can be written as

$$Y(t_{i+1}) \approx \exp(hJ(x(t_i)))Y(t_i) \tag{12}$$

and finally we have

$$Y(T) = \lim_{h \rightarrow 0} \prod_{i=0}^{M-1} \exp(hJ(x(t_i))). \tag{13}$$

By using this equation, the description of the numerical Lyapunov exponents at time T can be written in the form

$$\lambda_i = \frac{1}{T} \sum_{j=0}^{M-1} \ln(R_j)_{i,i}. \tag{14}$$

We set $L \geq 1$ and $\frac{M}{L} > 1$ in order to apply the Gram-Schmidt reorthonormalization procedure to each product $\prod_{i=jL}^{jL+L-1} \exp(hJ(x(t_i)))$ instead of the single term $\exp(hJ(x(t_i)))$ where j is an integer. So Gram-Schmidt reorthonormalization procedure is applied once only for every time length Lh and the computation time reduces. The matrix exponential is computed approximately by using the truncated Taylor expansion:

$$\exp(hJ(x)) \approx I_n + \sum_{i=1}^{16} \frac{h^i}{i!} J(x)^i \tag{15}$$

The numerical time integration used to discretize Eq. (1) is performed by using a linear multi-step method given by the fourth-order Adams-Bashforth formula[18,19]:

$$x_{n+1} = x_n + \frac{h}{24} [55f(x_n) - 59f(x_{n-1}) + 37f(x_{n-2}) - 9f(x_{n-3})]. \tag{16}$$

3.2 Construction of The Jacobian Matrix

When considering such a dynamical system, it is a straightforward procedure to construct the Jacobian matrix of differential equation that characterizes the system. To do this we need to convert our non-autonomous system to an autonomous system. As mentioned earlier in this section, a non-autonomous system of equation that describes the evolution of the dynamical system can be rewritten as an autonomous system by adding an equation. The differential equation that describes the blade-disk-shaft system has already been given as Eq.(5) in previous section, which has τ as a dimensionless time variable. One can rewrite the differential equation of the system, i.e., Eq.(5) as a

system of equations by making a new substitution $x' = y$. Then it becomes a set of first order ODE's

$$\begin{aligned}x' &= y \\y' &= -f(\tau)x \\ \tau' &= 1,\end{aligned}$$

where prime denotes differentiation with respect to τ and the function $f(\tau)$ is the fractional part of second term of the left-handside of Eq.(5). The third equation above guarantees that the system is autonomous. To clarify system of equations, it is suitable to make a transformation $x \rightarrow x_1, y \rightarrow x_2, \tau \rightarrow x_3$. Then, the blade-disk-shaft system can be represented as a matrix equation. We have

$$\begin{pmatrix} x_1' \\ x_2' \\ x_3' \end{pmatrix} = \begin{pmatrix} 0 & 1 & 0 \\ -f(x_3) & 0 & 0 \\ 0 & 0 & 1/x_3 \end{pmatrix} \begin{pmatrix} x_1 \\ x_2 \\ x_3 \end{pmatrix}. \quad (17)$$

The jacobian matrix can be constructed as 2×2 matrix taking the first and second rows and columns of the matrix seen righthandside of Eq.(17) i.e.,

$$J = \begin{pmatrix} 0 & 1 \\ -f(x_3) & 0 \end{pmatrix} \quad (18)$$

which actually represents the evolution of our dynamical system. Certainly, this representation is an irreducible one.

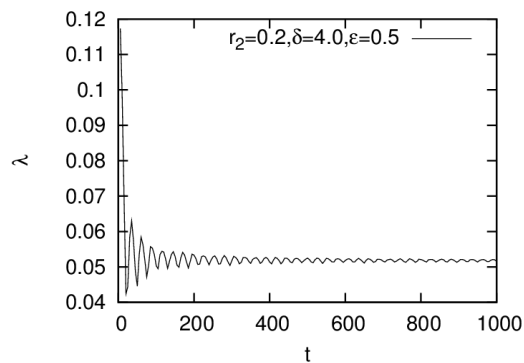


Figure 3. The LCE λ calculated for a given specific parameter set.

3.3 Computing The LCE's

Each Lyapunov exponent has been calculated by employing a routine code whose step size h is set to 0.01. This value of h is sufficiently small to use when compared to other studies. A subroutine inside code has been utilized to numerical integration including forth-order Adams-Bashford formula (see Eq.16). This provides high precession in computations.

Table 1. The sign of LCEs

Topological Dimension	Trajectory of Attractor	Sign of LCE (λ)
1	Fixed Point	-
2	Periodic Motion	0,-
3	Torus T^2 , Chaos C^1	00-,+0-

4. Stability and Unstability Regions

In determining the stability regions of the dynamical system under consideration, it is useful to deal with outcomes of strained parameter method [20]. The method is used in calculating the branches separating stable and unstable regions, which is based on perturbation analysis. In Eq.(5), one can observe that there are, in fact, three parameters (δ, ε, r_2) that govern the stability of dynamical system.

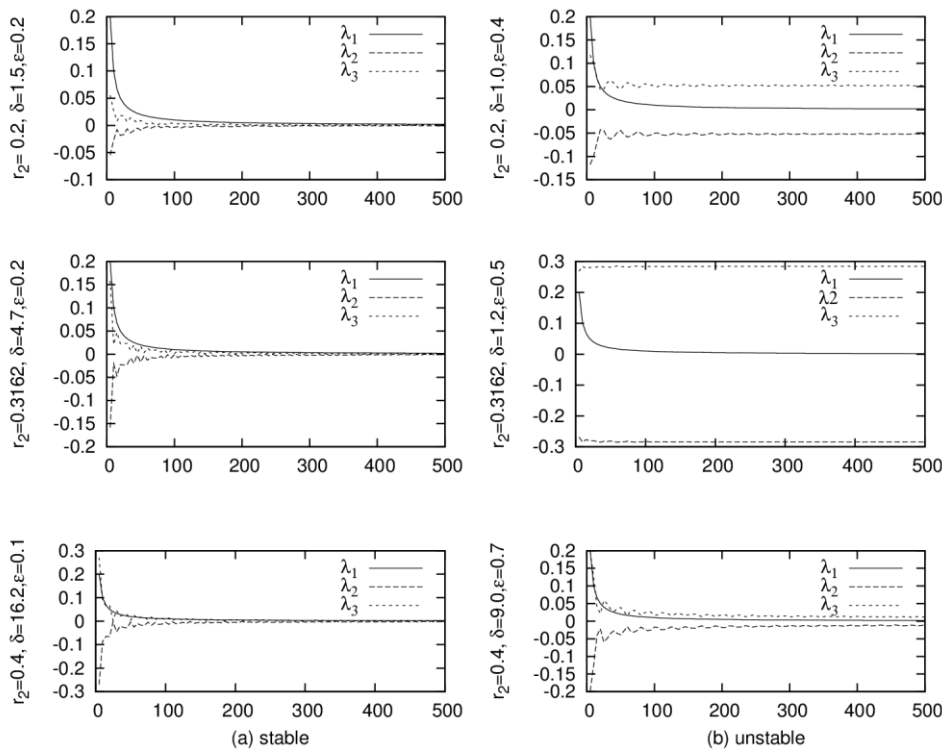


Figure 4. The LCEs $\lambda_1, \lambda_2, \lambda_3$ at selected points in stable (a) and unstable (b) regions of the grid.

Parameter Space: An approximate analytical solution of Eq.(5) given by Al-Nassar et al. (2007) may guide our analysis to estimate stability and instability regions of the differential equation of system under consideration. According to [8], parameter r_2 should be not very small or large ($r_2 \approx 0$). The stability branches seem to emerge from specific values of $\delta = 0, 1, 4, \dots, n^2$ where n is an integer while parameter ε varies between 0 and 1. Thus, the parameter space is constructed as $\delta - \varepsilon$ grids. Then the LCE's is now to be computed for every points of parameter space in which each of points represent a dynamical system state mentioned in section 3. As an example, the time evolution of a LCE has been plotted in Fig.3 for a specific set of parameters. If sufficiently long time is passed it converges a limit value.

The stability of a point in the space is determined by the sign of LCEs given in Table 1. The dimension of dynamical system considered is 3. Thereby three Lyapunov exponents will occur,

namely here λ_1, λ_2 and λ_3 ; at least one of these tends always to go monotonically to zero as seen in Fig.4 (say, $\lambda_1 \rightarrow 0$). In stable regions, it is well known that at least one of LCEs is zero when the trajectory of an attractor has no fixed points [21]. If there is at least one positive exponent then the system has a strange attractor, thus has a chaotic behavior (See Fig.4 (b)). For a system having positive Lyapunov exponents ($\lambda_i > 0, \exists i$), it is said to be chaotic. This means that the differential equation of the system would have some instability regions. Here in our study, the LCE whose value approaches positive numbers is just λ_3 as shown in Fig.4, and thus it is expected that the system considered will exhibit chaotic behavior.

5. Results and Discussion

As mentioned above, the differential equation that represents our system would have both stability and instability regions. The LCEs were computed for every points of $\delta - \varepsilon$ grids in parameter space. The dimensionality of our dynamical system is set to 3, hence there are three LCEs to compute for each points of grid. According to our results, it is possible to say that the exponent corresponding to time variable should approaches rapidly to zero ($\lambda_1 \rightarrow 0$) and produces a limiting cycle in the motion of the dynamical system. It is also seen that the 2nd LCE (λ_2) produces dominantly periodic motions due to its non-positive values. Only the 3rd LCE λ_3 takes positive values for specific parts of the grid and therefore is responsible for chaotic motion of the system.

In this paper, we aimed to investigate the stability branches in the scope of LCEs and paid more attention to λ_3 which seem to be the source of chaotic behavior. In Figs.(5-7), positive values of λ_3 representing by “+z-axis” refer to unstable region and zero surfaces correspond to stable region. At first glance, it is easy to see that for different r_2 values there are resembling patterns in $\delta - \varepsilon$ grids for Figs.(5-7). In all figures, the half funnel-shaped surfaces illustrate the positive Lyapunov exponents. Thus, points on those surfaces belong to the unstable region of the system driven by shaft torsional vibration.

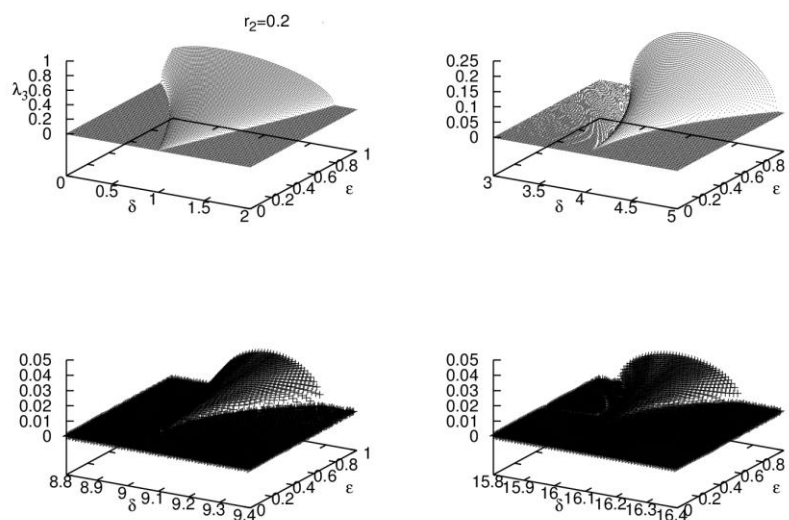


Figure 5. The LCE λ_3 in the $\delta - \varepsilon$ grid for $r_2 = 0.2$ with $n=1,2,3,4$.

Fig.5 shows four landscapes for r_2 . The specific value of δ that determines stability branches according to n^2 (where n in an integer) is set to 1,2,3, and 4 respectively. The grid step size is chosen as 0.01 for both variables ε and δ . Thus, there are exactly $200 \times 100 = 20000$ points in the region $\delta \in [0,2]$ and $\varepsilon \in [0,1]$ for first landscape of the figure. In the second landscape, boundaries of region are $\delta \in [3,5]$ and $\varepsilon \in [0,1]$ respectively, which includes equally amount of points with first landscape. Third and fourth landscapes have less amount of points and thus have less density. In Figs.6 and 7, similar landscapes are observed. In both, the first landscape of figures is seen to be much dense because of the intensity of points. In these cases,

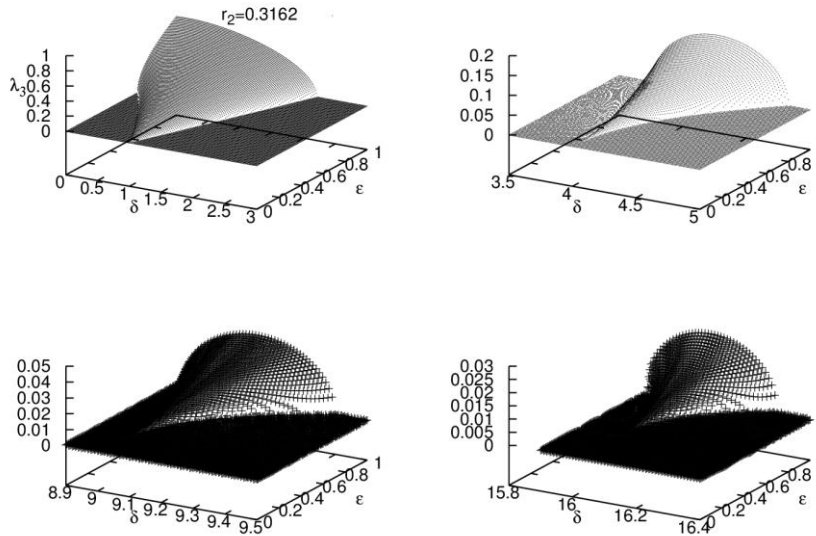


Figure 6. The LCE λ_3 in the $\delta - \varepsilon$ grid for $r_2 = 0.3162$ with $n = 1, 2, 3, 4$.

the parameter r_2 takes the values of 0.3162 and 0.4, respectively. In the third and especially fourth landscapes of figures, the intensity of fluctuations of 3th LCE around zero becomes more evident due to the relative intensity of the value of λ_3 . Outside of the aforementioned specific surfaces, some additional set of points making λ_3 positive are obtained. This set also corresponds to instability. The values of λ_3 in first landscapes in both figures are obviously greater than those in the other landscapes. This means that the chaotic behavior of the attractor of the system arises relatively more intensive near the value of parameter $\delta = 1$. The boundaries between half-funnel shapes and flat surfaces in figures might be interpreted as transition zones indicating the edge of chaos. If a cross-section is taken near the zero surface for each figure then in corresponding regions, an excellent agreement is obviously observed with the study done in [8].

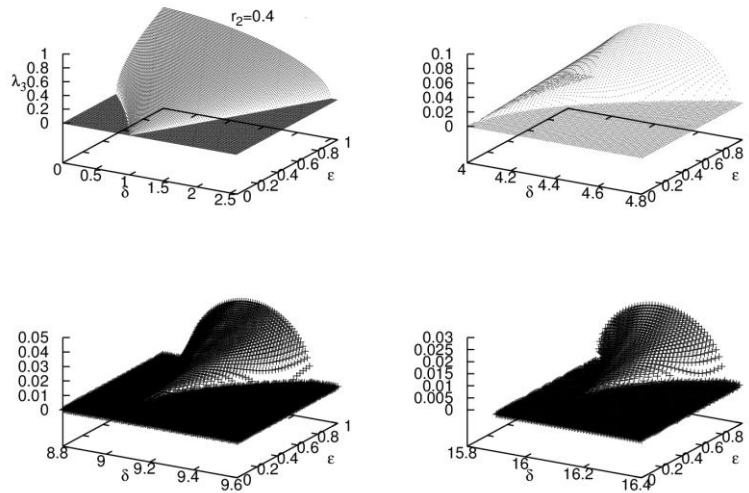


Figure 7. The LCE λ_3 in the $\delta - \epsilon$ grid for $r_2=0.4$ with $n = 1,2,3,4$

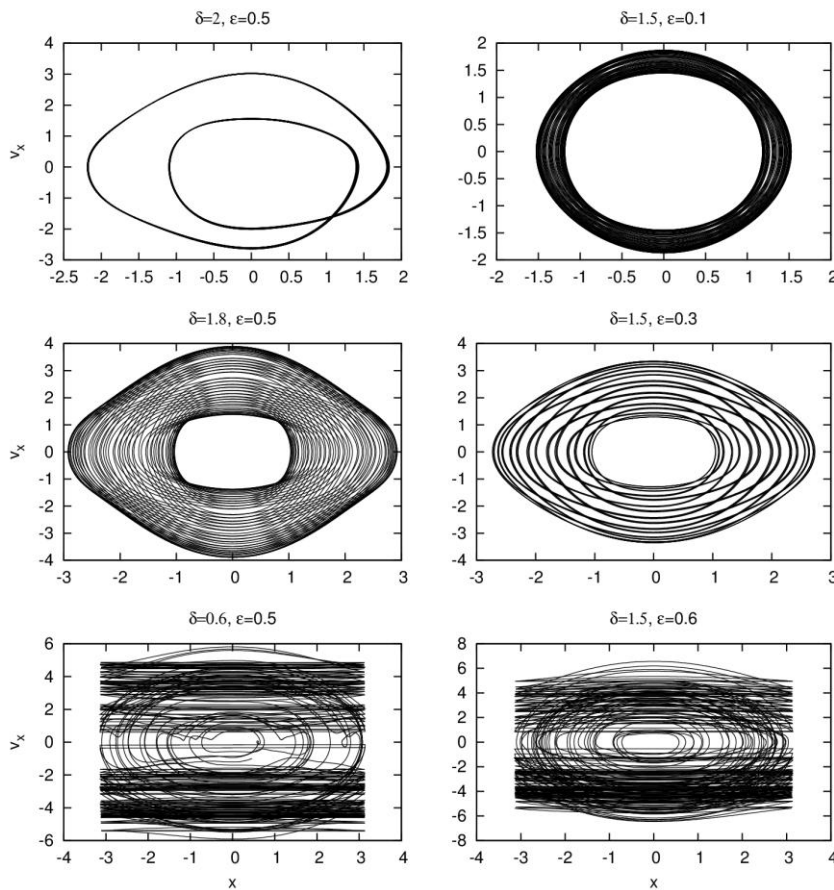


Figure 8. Phase space trajectories of a landscape of the grid where parameters $r_2=0.2$ and $n = 1$.

To make a more distinct explanation for the instability regions of the system, one can draw the phase space trajectories. Such trajectories are known as attractors in the phase space of dynamical systems as briefly explained in Sec.4. In Fig.8 trajectories have been plotted for the dynamical system under consideration. The parameter set is chosen for two different regions as expected; while imaginary vertical and horizontal paths are followed in $\delta - \varepsilon$ grid for a selected landscape for example, one can meet specifically three cases. In the first case, we are in region where all LCEs are zero; namely we are in a stable region. The first row of Fig.8 shows this case. Attractors strongly resemble limiting cycles referred to periodic motions of the system. The second case is related to transition zones where torus-shaped trajectories occurred according to Table 1. In this case, λ_2 is negative we are faced to edge of chaos because, attractors drawn on the second row of the figure begin apparently to show quasi-periodic cycles which may be interpreted as escaping from the regular motion. In the third case, attractors become strange where we are now in an unstable region of the grid. Here, λ_3 is strictly positive and chaotic behavior is observed.

6. Conclusion

In this paper, we focused on reestablishing an analysis for the stability and instability regions of rotating blade vibration due to shaft torsional excitation in terms of Lyapunov exponents. To do this, one can rewrite the second order differential equation as two coupled first order differential equations. This enables us to develop necessary tools for generating the Lyapunov exponents.

The LCEs are distinctly essential indicators for understanding the evolution of dynamical systems. Here we have three LCEs one of which is systematically zero. One of remaining takes negative values and the latter one takes positive values for unstable regions as shown in figures. For special sections of parameter space (grid), landscapes are built up where unstable regions are exhibited by the intensity of third LCE λ_3 . When comparing the instability of regions studied by "strained parameter method" described by Al-Nassar [8] with those which are found in this work, a close match is observed.

Moreover, the phase space trajectories of the corresponding sections are plotted for different parameter sets to illustrate how the dynamical system evolves. The trajectories are as known, called attractors. In stable regions of a typical section, attractors are found to depict periodic motions as shown in Fig.8 whereas in unstable regions, they begin to depict chaotic motions which is unpredictable, and turn out to be strange attractors. At the boundaries that two regions are met, we observe the phase transition which means the system is in the edge of chaos.

References

- [1] Srinivasan, A.V., "Vibrations of bladed-disk assemblies: a selected survey", Journal of Vibration and Acoustics, 1984, 106 : 165-168.
- [2] Crawley, E. F., Mokadam, D. R., "Stagger angle dependence of inertial and elastic coupling in bladed disks", ASME Journal of Vibration, Acoustics Stress and Reliability in Design, 1984, 106: 181-188.
- [3] Tang, D., Wang, M., "Coupling technique of rotor-fuselage dynamic analysis", ASME Journal of Vibration and Acoustics, 1984, 106: 235-238.
- [4] Okabe, A., Otawara, Y., Kaneko, R., Matsushita, O., Namura, K., "An equivalent reduced modeling method and its application to shaft-blade coupled torsional vibration analysis of a turbine-generator set", Proceedings of Institute of Mechanical Engineers, 1991, 205: 173-181.
- [5] Huang, S., Ho, K., "Coupled shaft-torsion and blade-bending vibrations of a rotating shaft-blade unit", Journal of Engineering for Gas Turbines and Power, 1996, 118: 100-106.

- [6] Al-Bedoor, B.O., "Reduced-order nonlinear dynamic model of coupled shaft-torsional and blade-bending vibrations in rotors", *Journal of Engineering for Gas Turbines and Power*, 2001, 123: 82-89.
- [7] Al-Nassar, Y. N., Al-Bedoor, B. O., "On the vibration of a rotating blade vibration on a torsionally flexible shaft", *Journal of Sound and Vibration*, 2003, 259: 1237–1242.
- [8] Al-Nassar, Y. N., Kalyon, M., Pakdemirli, M., Al-Bedoor, B. O., "Stability Analysis of Rotating Blade Vibration due to Torsional Excitation", *Journal of Vibration and Control*, 2007, 13: 1379-1391.
- [9] Chen, Z. M., et al., "Computing Lyapunov exponents based on the solution expression of the variational system", *Appl. Math. Comput.*, 2006, 174: 982-996.
- [10] Al-Bedoor, B. O., Al-Qaisia, A. A., "Stability analysis of rotating blade bending vibration due to torsional excitation", *Journal of Sound and Vibration*, 2005, 282: 1065-1083.
- [11] Sandri, M., "Numerical calculation of Lyapunov Exponents", *The Mathematica Journal*, 1996, 3: 78-84.
- [12] Wolf, A., Swift, J. B., Swinney, H. L., Vastano, J. A., "Determining Lyapunov exponents from a time series", *Physica D*, 16 (1985) 285-317.
- [13] Geist, K., Parlitz, U., Lauterborn, W., "Comparison of different methods for computing Lyapunov exponents", *Prog. Theor. Phys.*, 1990, 83: 875-892.
- [14] Oseledec, V. I., "A multiplicative ergodic theorem. characteristic Lyapunov exponents of dynamical systems", *Trans. Moscow Math. Soc.*, 1968, 19: 197-231.
- [15] Benettin, G., Galgani, L., Giorgilli, A., Strelcyn J. M., "Lyapunov characteristic exponents for smooth dynamical systems and for Hamiltonian systems; a method for computing all of them", Part I and Part II, *Meccanica*, 1980, 15: 9-30.
- [16] Christiansen, F., Rugh, H. H., "Computing Lyapunov spectra with continuous Gram–Schmidt orthonormalization", *Nonlinearity* 1997, 10: 1063-1072.
- [17] Lu, J., Tang, G., Oh, H., Luo, A. C. J., "Computing Lyapunov exponents of continuous dynamical systems: method of Lyapunov vectors", *Chaos Solitons Fract.* 2005, 23: 1879-1892.
- [18] Moler, C., Van Loan, C., "Nineteen dubious ways to compute the exponential of a matrix, twenty-five years later", *SIAM Rev.*, 2003, 45: 3-49.
- [19] Lambert, J. D., "Numerical Methods for Ordinary Differential Systems", Wiley, Chichester (1991).
- [20] Nayfeh, A. H., "Introduction to Perturbation Techniques", Wiley, New York, (1981).
- [21] Haken, H., "At least one Lyapunov exponent vanishes if the trajectory of an attractor does not contain a fixed point", *Phys. Lett. A*, 1983, 94: 71.